Identification of Actin-, α-Actinin-, and Vinculin-containing Plaques at the Lateral Membrane of Epithelial Cells

Detlev Drenckhahn and Henning Franz

Institute of Anatomy and Cell Biology, University of Marburg, D3550 Marburg, West Germany

Abstract. In this paper, a new type of spot desmosome-like junction (type II plaque) is described that is scattered along the entire lateral plasma membrane of rat and human intestinal epithelium. Ultrastructurally type II plaques differed from the classical type of epithelial spot desmosome ("macula adherens", further denoted as type I desmosome) by (*a*) weak electron density of the membrane-associated plaque material, (*b*) association of the plaques with microfilaments rather than intermediate filaments, and (*c*) poorly visible material across the intercellular space. Thus, type II plaques resemble cross-sections of the zonula adherens. Immunofluorescence-microscopic studies were done using antibodies to a main protein associated with the plaques of type I desmosomes (desmoplakin I) and to the three major proteins located at the plaques of the zonula adherens (actin, α-actinin, and vinculin). Two types of plaques were visualized along the lateral surface of intestinal and prostatic epithelium: (*a*) the type I desmosomes, which were labeled with anti-desmoplakin but did not bind antibodies to actin, α-actinin, and vinculin, and (*b*) a further set of similarly sized plaques, which bound antibodies to actin, α-actinin, and vinculin but were not stained with anti-desmoplakin. Three-dimensional computer reconstruction of serial sections double-labeled with anti-desmoplakin and anti-α-actinin further confirmed that both types of plaques are spatially completely separated from each other along the lateral plasma membrane. The computer graphs further revealed that the actin-, α-actinin-, and vinculin-containing plaques have the tendency to form clusters, a feature also typical of type II plaques. It is suggested that the type II plaques represent spot desmosome-like intercellular junctions, which, like the zonula adherens, appear to be linked to the actin filament system. As the type II plaques cover a considerable part of the lateral cell surface, they might play a particular role in controlling cellular shape and intercellular adhesion.

EPITHELIA of a number of cavity organs and exocrine glands are linked to each other by different types of intercellular junctions. These junctions can be grouped into (*a*) tight junctions, which seal the intercellular space and form a permeability barrier, (*b*) communicating junctions (gap junctions), which mediate transcellular passage of smaller molecules, and (*c*) adhering junctions, which hold the cells mechanically together (for reviews, see references 1, 32, 36, and 42).

The adhering intercellular junctions, desmosomes, occur in two different forms: belt desmosomes (zonula adherens) and spot desmosomes (macula adherens). Belt desmosomes surround each of the interacting cells close to the cell apex (13). The intercellular space contains bridging filaments, which are well visible in deep etch images (25), but are less readily seen in thin sections of conventionally fixed and stained sections (13, 27). Previous studies indicated that uvomorulin, an adhesive embryonic glycoprotein, is present in the intercellular space of the zonula adherens (3). The cytoplasmic aspect of the belt desmosomes is characterized by a contractile bundle of actin filaments (39) that extend circumferentially along the cytoplasmic surface of the junctional membrane (5, 26). Immunocytochemical studies have demonstrated α-actinin and vinculin, two actin filament-associated proteins, to be concentrated at the cytoplasmic aspect of belt desmosomes (20, 21). Vinculin appears to be closer to the plasma membrane than is α-actinin. Since vinculin and α-actinin are major components of certain types of actin filament-membrane associations (19, 29), it is generally assumed that both proteins are important for the anchorage of actin filaments to the plasma membrane.

In contrast to the belt desmosomes, spot desmosomes are scattered along the entire lateral cellular surface and appear to act like rivets holding the cells together. The intercellular space between the interacting membranes contains bridging filaments, characteristically forming an electron-dense midline located halfway between the opposed membranes (27, 32, 42). On the cytoplasmic side are electron-dense plaques 10–20-mm thick. These plaques are associated with bundles of intermediate filaments (tonofilaments) which, in epithelial

cells, are composed of cytokeratin polypeptides (18). Isolated spot desmosomes consist of several glycoproteins that are thought to be located in the intercellular cleft. In addition, proteins at M_r ~ 82,000, ~ 215,000, and ~ 250,000 D were detected, which appear to be constituents of the cytoplasmic plaques (17, 22). This location has been clearly demonstrated for the M_r ~ 250,000 (desmoplakin I) and M_r 215,000 (desmoplakin II) components (17).

In a previous study on the cytoskeleton of exocrine gland cells, we observed that antibodies to actin and α-actinin displayed an interrupted patchy staining pattern that extended along the entire basolateral plasma membrane (12). This pattern indicated the existence of multiple spot-like membrane specializations probably not related to the tonofilament-associated spot desmosomes. In support of this view we now present evidence that epithelial cells contain a second set of spot desmosome–like intercellular junctions (type II plaques) that differ structurally and biochemically from the tonofilament-associated spot desmosomes (type I desmosomes). Like the zonula adherens, type II plaques appear to be associated with actin, α-actinin, and vinculin and do not contain desmoplakins, the marker proteins of type I desmosomes. It is suggested that the system of type II plaques serves to mechanically couple the cytoplasmic contractile filament system to the basolateral cell membrane.

Materials and Methods

Electron Microscopy

Small pieces of the human and rat duodenal mucosa taken during narcosis were fixed for 1 h at 4°C by immersion in either 2% glutaraldehyde in phosphate-buffered (20 mM) saline (125 mM) (PBS, pH 7.4) or in a fixative that contained 1% glutaraldehyde, 2% tannic acid, and 0.1% saponin (30). After several washes with PBS (6 changes, 2 h), samples were postfixed for 1 h with ice-cold 1% OsO_4 in PBS, dehydrated in graded ethanol series immersed with propylene oxide, and embedded in Epon 812. Ultrathin sections (50–100 nm) were counter-stained with lead citrate and uranyl acetate and examined with a Zeiss EM 10 electron microscope.

Fluorescence Microscopy

Tissue pieces (~1 mm^3) were rapidly frozen in melting isopentane (cooled with liquid nitrogen). The frozen tissue samples were carefully freeze-dried for 12 h each at −90°C, −40°C, −20°C, 0°C, and +20°C at a vacuum of 10^{-5} Torr, then placed for 48 h at 10^{-3} Torr (20°C) in Epon that contained 1.8% (vol/vol) Epon accelerator and then placed in gelatin capsules and polymerized at 60°C for 24–48 h. Semithin tissue sections (0.3–1 μm) were mounted on glass slides and prepared for immunostaining as described (11, 12). Removal of the resin was done by placing the slides for 5–15 min in a methanol-toluene solution that contained 10% sodium methoxide (prepared from metallic sodium as described, 31). Finally, the sections were rinsed with a 1:1 mixture of methanol and toluene (5 min), acetone (2 × 5 min), distilled water (2 × 5 min), and PBS (pH 7.4) that contained 2% bovine serum albumin (BSA) (15 min). Antibody incubation was done by overlaying each section for 30 min at 20°C with 40 μl of primary antiserum (diluted 1:40 in PBS) or affinity-purified IgG (~10 μg/ml in PBS). After a 30 min wash with PBS, sections were incubated for 30 min at 20°C with either rhodamine- or fluorescein-labeled goat anti-rabbit IgG diluted with PBS (1:40), then washed with PBS (30 min), and mounted in 50% glycerol in PBS that contained 1.5% *n*-propyl gallate to reduce fading of fluorescence. Binding sites of two different antibodies in the same section were determined by a sequential staining technique. The staining pattern obtained with the first antibody was photographed and then eliminated by removing the IgGs with 0.05% $KMnO_4$ in 0.1% H_2SO_4 for 10 s followed by exposure to 0.5% $Na_2S_2O_5$ for 5–10 s (45). After the section had been checked for complete removal of the previous stain (always the case under these modified conditions), they were reincubated with another antibody and photographed again. Staining with rhodamine-labeled phalloidin (specific probe for polymerized actin; 14) was done using cryostat sections of human duodenal mucosa fixed with 2% paraformaldehyde in PBS (30 min), rinsed with PBS that contained BSA (2 h), and soaked with 18% sucrose in PBS as described (9).

Controls were done in which the antibodies were replaced by (*a*) preimmune serum (1:10 dilution), (*b*) antibodies to actin, α-actin, and vinculin absorbed with an excess of their respective antigen, or (*c*) anti-desmoplakin absorbed with isolated desmosomal plaques. The phalloidin stain was controlled by a 1:10 mixture of rhodamine-phalloidin and unlabeled phalloidin (Boehringer Mannheim GmbH, Mannheim, FRG).

Antibodies, Heat Elution of Affinity-purified IgGs

Antibodies to actin (23), α-actinin (15), and vinculin (12) from chicken gizzard, α-actinin from chicken pectoral muscle (12), and desmoplakin I from cow snout stratum spinosum (17) were prepared according to the references indicated and checked by Western blot analysis (Fig. 1). Antibodies were affinity-purified using the respective antigens immobilized by transfer to nitrocellulose paper (43). The bound IgGs were eluted by a 30-min incubation of the nitrocellulose sheets with 56°C PBS. This kind of heat elution of the bound IgG was found to be superior to elution with 0.2 M glycine-HCl (pH 2.8), as judged by the intensity of fluorescence obtained with IgGs eluted by both procedures.

Immunoblotting Studies

Human intestinal epithelium was isolated by a 30-min incubation of duodenal mucosa with an ice cold buffer that contained 100 mM NaCl, 8 mM KH_2PO_4, 6 mM Na_2HPO_4, 1.5 mM KCl, and 10 mM EDTA, pH 6.8. After gentle scraping with a rubber policeman, detached cells were collected at 400 *g* at 10 min and washed three times in the same buffer. Tonofilament-associated desmosomes were isolated from bovine snout stratum spinosum cells using the citric acid–sodium citrate method, which includes final purification on a discontinuous sucrose gradient (41). Isolated intestinal epithelium and desmosomes were directly dissolved in sample buffer according to Laemmli (28) and subjected to sodium dodecyl sulfate polyacrylamide gel electrophoresis in the presence of 2% β-mercaptoethanol. The separated protein bands were electrophoretically transferred to nitrocellulose paper (6) (Schleicher & Schull, Darmstadt, FRG), which was then processed for antibody staining using the peroxidase, anti-peroxidase method as described (11).

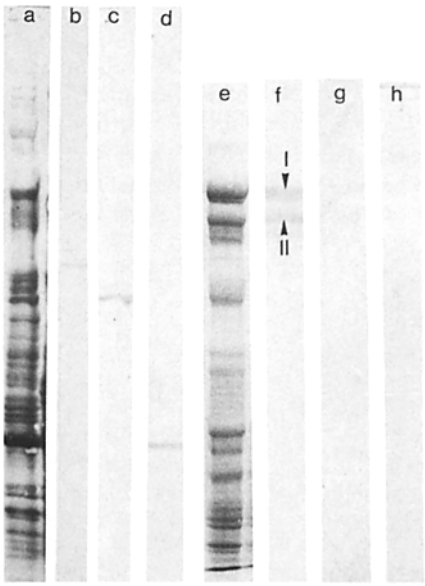

Figure 1. Specificity of antibodies as determined by Western blot analysis of isolated whole human intestinal epithelium (*a–e*) and crude desmosome preparation of bovine snout epithelium (*e* and *f*). Proteins were electrophoretically separated by $NaDodSO_4$ polyacrylamide gradient gels (*a–d*: 5–10%; *e–f*: 5–7.5% acrylamide) and transferred to nitrocellulose paper. Lanes were stained with either Amido black (*a* and *e*) or incubated with antibodies to vinculin (*b* and *h*), α-actinin (*c* and *g*), actin (*d*), or desmoplakin I (*f*). Antibodies are monospecific for protein bands of the same apparent molecular weight as the respective antigens. Arrowheads indicate polypeptide bands corresponding to desmoplakins I and II.

Results

Immunoblotting

In homogenates of human intestinal epithelium, antibodies to actin, α-actinin, and vinculin bound to polypeptide bands of M_r ~ 42,000, ~ 100,000, and ~ 120,000, respectively. No other cross-reactive polypeptide bands were detected by this method (Fig. 1, *a–d*). In crude desmosome preparations of the bovine snout, anti-desmoplakin I reacted with both desmoplakins I and II as previously reported (17). Anti-vinculin and anti-α-actinin did not bind to any polypeptide in the desmosome fraction (Fig. 1, *e–h*).

Electron Microscopy

The human intestinal epithelium is joined by a typical "junctional complex" (13), which was well visible in both the absence and presence of tannic acid in the fixative (Figs. 2 and 3). Under both fixation conditions, the intermediate filament (tonofilament)-associated spot desmosomes (further denoted as type I spot desmosomes) showed strongly electron dense cytoplasmic plaques (Figs. 2–5). The size of the desmosomes (defined as lateral extension of the plaques) ranged mostly between 50 and 150 nm. Close to the junctional complex, the size of individual desmosomes was up to 350 nm. The filamentous material that extended across the intercellular space of type I desmosomes was more intensely stained in the presence (Figs. 2, 3, and 5) than in the absence (Fig. 4) of tannic acid in the fixative. A typical midline structure was seen in many but not all sections of type I desmosomes. In the absence of tannic acid a small population of type I desmosomes showed only few detectable bridging filaments. Type I desmosomes were most frequently encountered in the apical half of the intestinal epithelium with the highest concentration close to the junctional complex.

In addition to type I desmosomes, a further type of similarily sized spot desmosome-like junction was observed in sections of both the human and rat intestinal epithelium (Figs. 2–5). These structures were found scattered along the entire lateral plasma membrane with apparently the same density in the apical as well as basal half of the cells. This type of spot desmosome-like junction (further denoted as type II plaque) was characterized by a rather low degree of electron density of the plaque material. The type II plaques were most clearly seen in sections of tissue fixed in the presence of tannic acid, but were also visible, albeit less obviously, in the absence of tannic acid. Unlike type I desmosomes the dense material of the type II plaques often did not form a continuous plaque. In many cases the type II plaques were composed of smaller subunits, 10–50 nm in size. This is well seen in Fig. 2, where type II desmosomes with continuous (zonula adherens-like) and discontinuous plaques are visible. As shown in Fig. 4, individual densities may be separated from each other by some hundred nanometers, giving rise to a group several individual small desmosome units (20–50 nm in size). Similar clusters of type II plaques were also seen in the rat intestinal epithelium.

At higher magnification most of the type II plaques showed a close relationship to a subplasmalemmal layer of thin filaments (diameter of the filaments 5–8 nm) which had the same morphology as the actin filaments associated with the zonula adherens (Figs. 3–5). Subplasmalemmal aggregates of microfilaments were most pronounced at places where the cells are interdigitated by lateral folds. In these interdigitating areas type II plaques were also observed at particular high density (Figs. 3 and 5).

The type II plaques were always arranged symmetrically, i.e., the plaques in one cell were associated with plaques of similar morphology located at the opposing membrane of the neighboring cells. The material present in the intercellular space between the type II plaques did not differ significantly from that of the zonula adherens and the remaining lateral cell surface. In tissue fixed in the presence of tannic acid, the entire intercellular space contained well stained material of granular and filamentous appearance (Figs. 2, 3, and 5). There was no obvious concentration of this fuzzy intercellular material in both the zonula adherens and type II desmosomes. However, in tissue samples fixed in the absence of tannic acid the intercellular space outside the junctions was more or less unstained, while at the level of both the zonula adherens and type II plaques some filamentous and granular material was seen across the intercellular space (Fig. 4).

Fluorescence Microscopy

Technical Consideration: Specificity of Staining in Striated and Smooth Muscle. As indicated by the ultrastructural data, type II plaques appear to be associated with actin-like filaments. Thus, a main concern of the present immunocytochemical studies was to determine whether actin and other major components of actin filament membrane associations, such as α-actinin and vinculin, co-distribute at the lateral plasma membrane of intestinal epithelium. Since the size of individual plaques was mostly <300 nm, a major technical demand was to use tissue sections thin enough to avoid superposition of individual desmosomes. Previous immunocytochemical studies on the localization of α-actinin in the intestinal epithelium (8, 20, 21) using cryotome sections of fixed and unfixed tissues obtained a rather weak staining along the lateral plasma membrane (for discussion of technical problems and artifacts see reference 8). Therefore, in this study, immunostaining was applied to 0.2–0.5-μm-thick tissue sections of quick-frozen, freeze-dried, and plastic-embedded tissue. The specificity and optical resolution of this technique is demonstrated in Figs. 6–11, which illustrate the immunocytochemical distribution of actin, α-actinin, and vinculin in 0.5-μm-thick plastic sections of smooth and striated muscle. Antibodies to actin labeled the muscular I-band and the whole cytoplasm of smooth muscle. Anti-α-actinin label was confined to the muscular Z-line (individual Z-discs were well revealed) and to spots located along the periphery and in the cytoplasm of smooth muscle cells (probably representing dense patches and dense bodies). Vinculin-like immunostain was located along the surface of striated muscle where Z-lines laterally join the membrane (typical site of "costameres"; 37). In smooth muscle, anti-vinculin displayed a typical "dense patch"- and "dense band"-like pattern (38) confined to the cellular periphery. These findings are fully consistent with the current view of the subcellular distribution of actin, α-actinin, and vinculin in smooth and striated muscle (24). This clearly documents the specificity and power of the technique used.

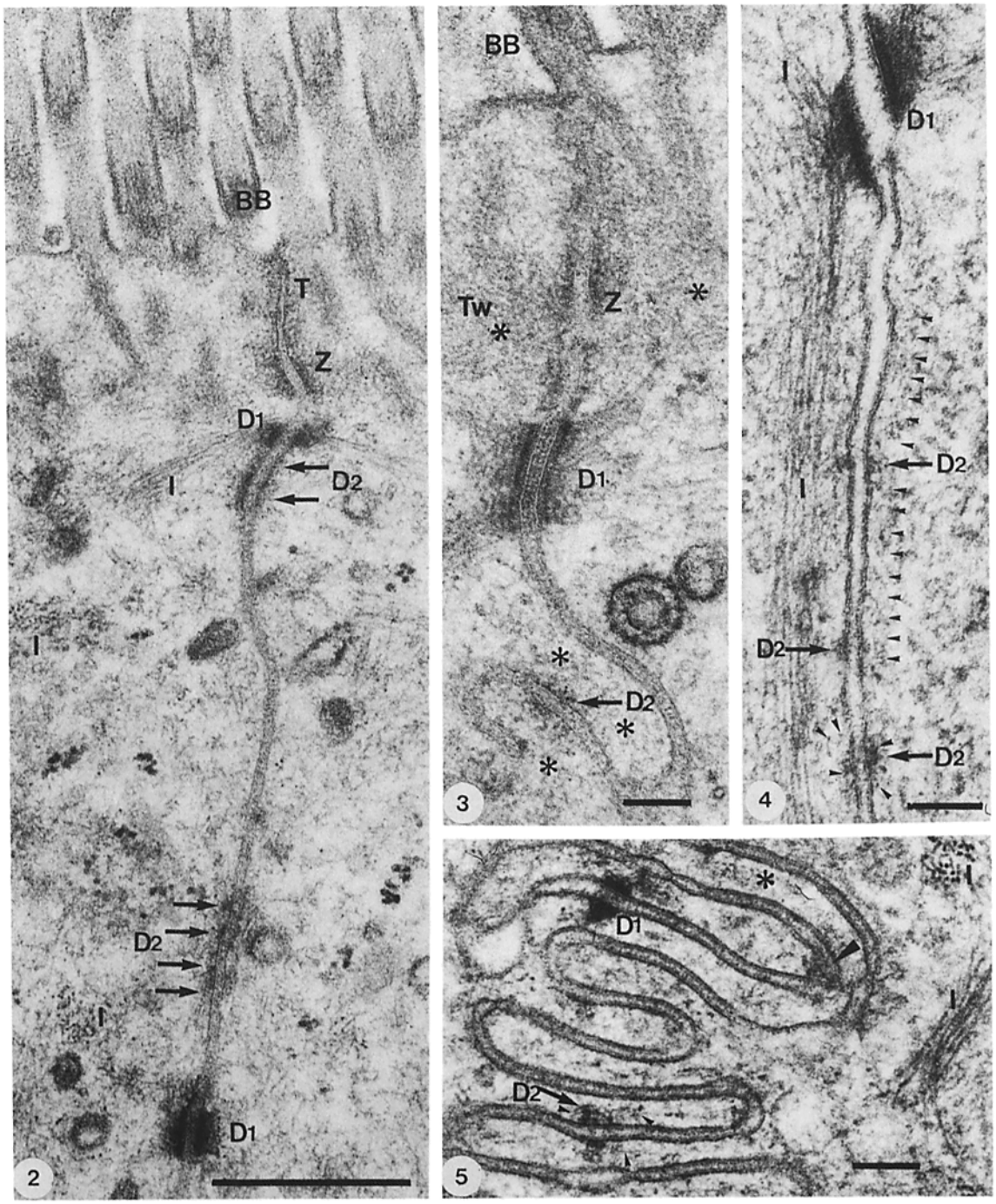

Figures 2–5. Electron micrographs of human intestinal epithelium fixed with glutaraldehyde in the presence (Figs. 2, 3–5) and absence (Fig. 4) of tannic acid. (Fig. 2) Apical portion of two neighboring cells (*BB*, brush border) joined by tight junctions (*T*), zonula adherens (*Z*), spot desmosomes (*D1*) and type II plaques (*D2*). The type I desmosomes (*D1*) are associated with bundles of intermediate filaments (*I*). Type II plaques (*D2*, arrows) are associated with microfilaments (not well seen at this magnification). Type II plaques with continuous (upper *D2*) and discontinuous, interrupted plaques (lower *D2*) are seen in this section. Bar, 0.5 μm. (Fig. 3) Similar area as shown in Fig. 2. Note microfilaments (asterisks) in association with the terminal web (*TW*) and both the zonula adherens (*Z*) and the type II plaques (*D2*, arrow). *D1* indicates a typical type I desmosome with a pronounced midline structure in the intercellular space. Bar, 0.1 μm. (Fig. 4) Cluster of type II plaques (*D2*, arrows) associated with a subplasmalemmal mat of microfilaments (small arrowheads). Note poorly stained fuzzy material in the intercellular space of type II plaques. Intermediate filaments (*I*) are associated with a type I desmosome (*D1*). Bar, 0.1 μm. (Fig. 5) Interdigitated part of the lateral cell surface showing profiles of type I desmosomes (*D1*) and type II plaques (*D2*, arrow). The large arrowhead points to a density probably belonging to a tangentially sectioned type II plaque. Asterisks and small arrowheads mark microfilaments clearly distinguished from intermediate filaments (*I*). Bar, 0.1 μm.

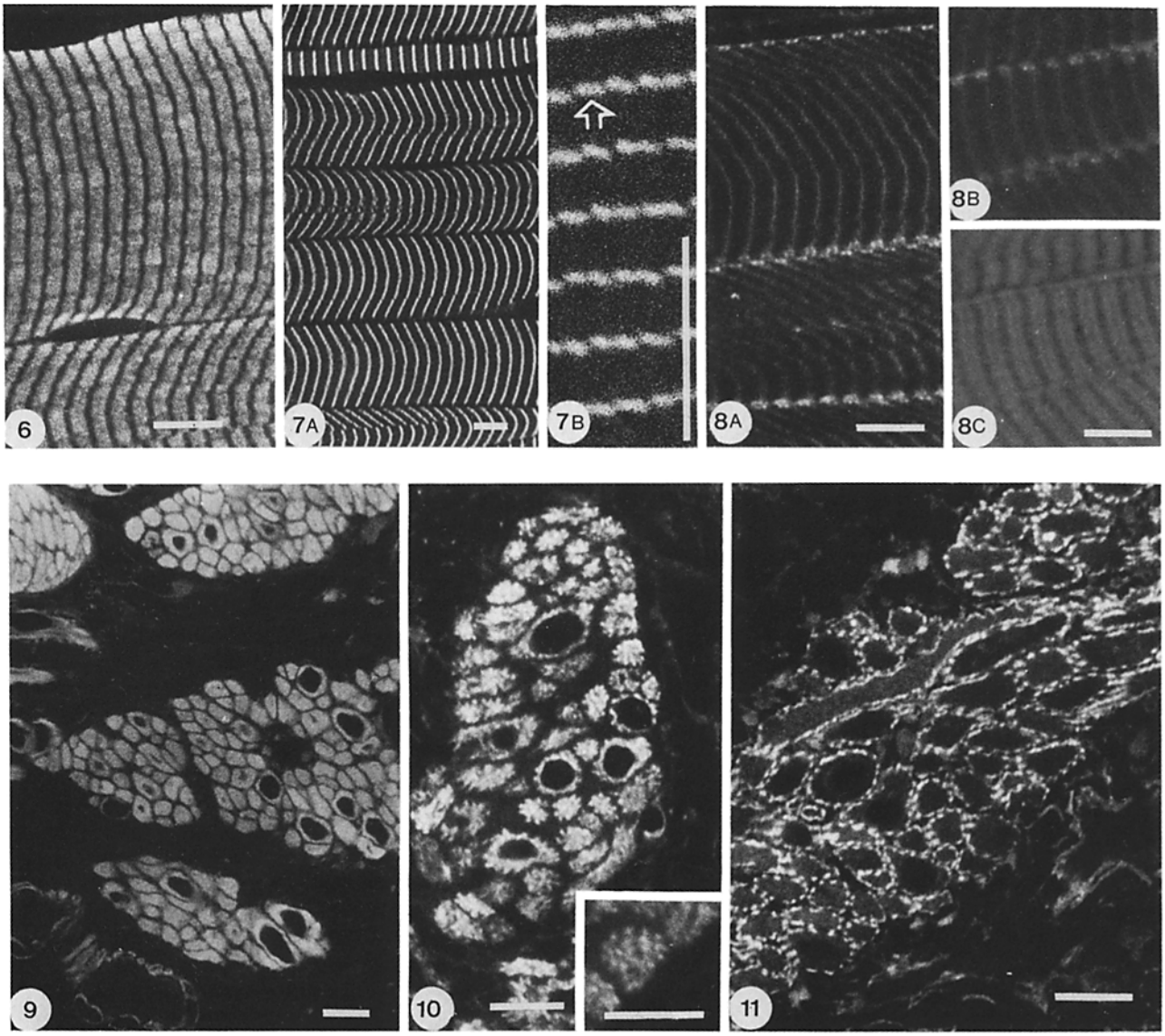

Figures 6–11. Specificity of antibody staining in semithin sections (0.5 μm) of quick-frozen, freeze-dried, and plastic-embedded striated muscle (Figs. 6–8) and intestinal smooth muscle (Figs. 9–11) incubated with antibodies to gizzard actin (Figs. 6 and 9), gizzard α-actinin (Fig. 7*A*), pectoral muscle α-actinin (Figs. 7 *B* and 10), and gizzard vinculin (Figs. 8 and 11). Striated muscle tissue was taken from rabbit psoas (Figs. 6 and 7*B*), mouse lumbrical (Fig. 7*A*), and chick posterior latissimus dorsi muscle (Fig. 8). Fig. 8 *C* is a phase contrast image of Fig. 8 *B*. Arrow in Fig. 7*B* points to individual Z-discs. Bar, 10 μm.

Intestinal Epithelium

Incubation of 0.3-μm plastic sections of human (and rat) intestinal epithelium with antibodies to actin, α-actinin, and vinculin resulted in an interrupted staining pattern that extended along the entire lateral plasma membrane (Figs. 13–16). Similar interruptions were also visualized in 1-μm-thick frozen sections of formaldehyde-fixed tissue incubated with fluorescently labeled phalloidin (Fig. 12). At favorite places where parts of the cells were cut parallel to the lateral membrane (tangential sections), small streak and dot-like plaques were seen scattered along the cell surface (Figs. 12 and 15). While the interrupted staining pattern associated with the lateral cell boundary was very similar with all three antibodies, conspicuous differences were noticed regarding the distribution of these proteins in the brush border region. These differences are in full agreement with previous immunocytochemical and ultrastructural studies on the intestinal brush border (4, 8, 10, 20, 21, 35): (*a*) Presence of actin in both the microvilli and the terminal webbs; (*b*) presence of α-actinin throughout the terminal webb region but its absence from microvilli; and (*c*) restriction of vinculin to the junctional complex (zonula adherens) (for reviews, see references 24 and 34).

Antibodies to desmoplakin produced a spotted staining pattern along the membrane (Fig. 17). The majority of spots were concentrated in the apical half of the epithelium as described previously for the intestinal epithelium of other vertebrates (7). At favorite places the spots could be further revealed to consist of two halves separated by a narrow line

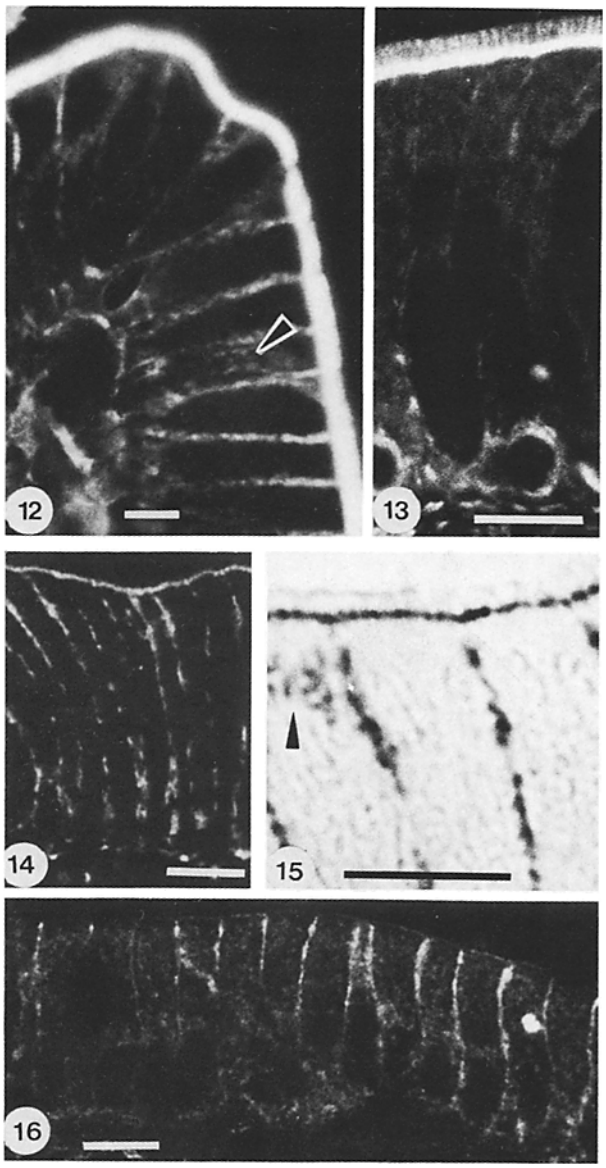

Figures 12–16. Cryostat (Fig. 12) and semithin plastic sections (Figs. 13–16) of human (Figs. 12–14, 16) and rat (Fig. 15) intestinal epithelium stained with rhodamine phalloidin (Fig. 12) and antibodies to actin (Fig. 13), gizzard α-actinin (Fig. 14), striated muscle α-actinin (Fig. 15, immunoperoxidase stain), and vinculin (Fig. 16). In all sections an interrupted staining pattern is seen along the lateral cell boundary. In tangentially sectioned cell walls (Figs. 12 and 15), irregularly shaped streaks and plaques are seen (arrowheads). Microvilli of the brush border and the terminal webb are stained with phalloidin and anti-actin. Anti-α-actinin labels the terminal webb region (interrupted stain) but not the microvilli. Vinculin is confined to the lateral cell membrane. Bar, 10 μm.

(Fig. 17 *b*). Obviously, this separating line represents the intercellular space, which is ~20-nm wide.

Double Labeling Studies on Intestinal and Prostatic Epithelium

To determine whether actin, α-actinin, and vinculin are co-localized within identical plaques along the lateral plasma membrane, cross-sectional areas of human intestinal epithelium were first labeled with anti-α-actinin and photographed. Then the immunostain was eliminated as described, and the sections were incubated with either anti-actin or anti-vinculin. As shown in Figs. 18 and 19, there was a high degree of co-location of α-actinin with either actin or vinculin. Similar results were obtained with rat prostatic epithelium (Franz, H., H.-J. Wagner, K. Schluter, and D. Drenckhahn, manuscript in preparation). Thus, actin, α-actinin, and vinculin are concentrated within the same type of plaque. These plaques were observed at rather high density along the entire lateral plasma membrane of the human intestinal and rat prostatic epithelium. When the same double-labeling experiments were done with antibodies to desmoplakin, a marker protein for type I desmosomes (vide supra), and α-actinin, clear-cut evidence was obtained that both types of plaques were spatially separated from each other (Fig. 20).

Three-dimensional Distribution of Type I Desmosomes and α-Actinin-containing Plaques

Serial 300-nm sections of human intestinal epithelial cells sequentially labeled with antibodies to α-actinin and desmoplakin were processed for three-dimensional computer reconstruction as described in Figs. 21 and 22. The computer graphs revealed further information not to be obtained by examination of individual sections. Type I desmosomes were more or less evenly distributed throughout the lateral cellular surface. This pattern is consistent with the pattern of type I desmosomes observed in tangential sections of the lateral cell mem-

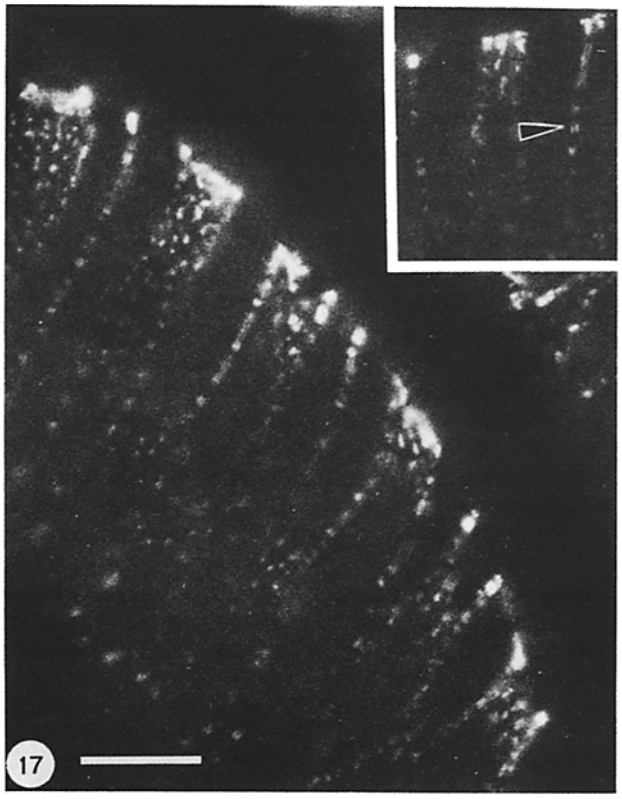

Figure 17. Visualization of type I desmosomes in 0.5-μm thick plastic sections of human intestinal epithelium incubated with anti-desmoplakin. Some plaques can be seen to be divided by an unstained narrow line (arrowhead). Bar, 10 μm.

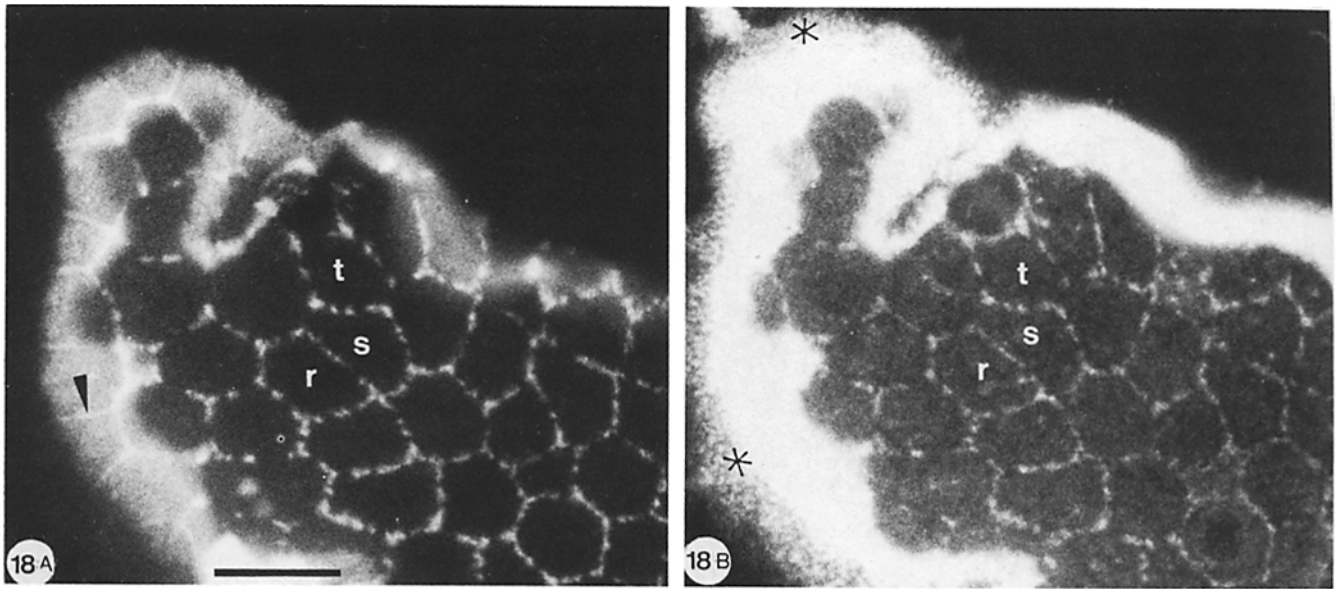

Figure 18. Same plastic section (cross-section) of the human intestinal epithelium stained sequentially with antibodies to α-actinin (*A*) and actin (*B*). Note co-distribution of both antibodies within the same plaques located at the lateral cell border. Microvilli (asterisks) are stained with anti-actin but not with anti-α-actinin. Arrowhead points to the zonula adherens. Some identical cells are marked by *r*, *s*, and *t*. Bar, 10 μm.

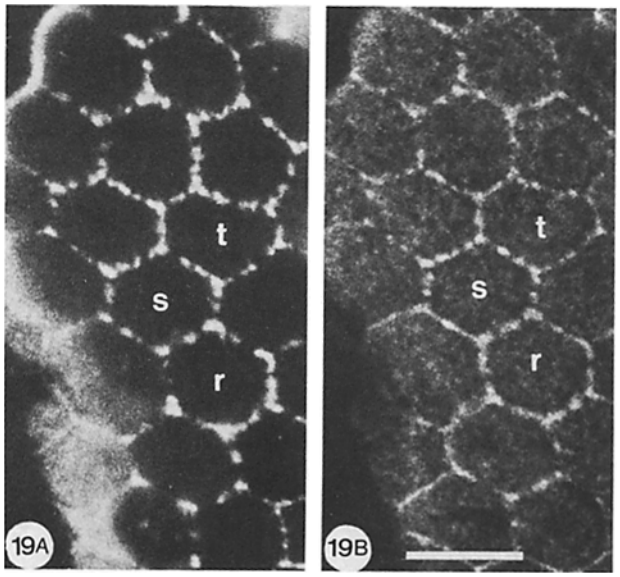

Figure 19. Codistribution of α-actinin (*A*) and vinculin (*B*) along the lateral cell border of human intestinal epithelium, including the zonula adherens. Some identical cells are labeled with *r*, *s*, and *t*. Bar, 10 μm.

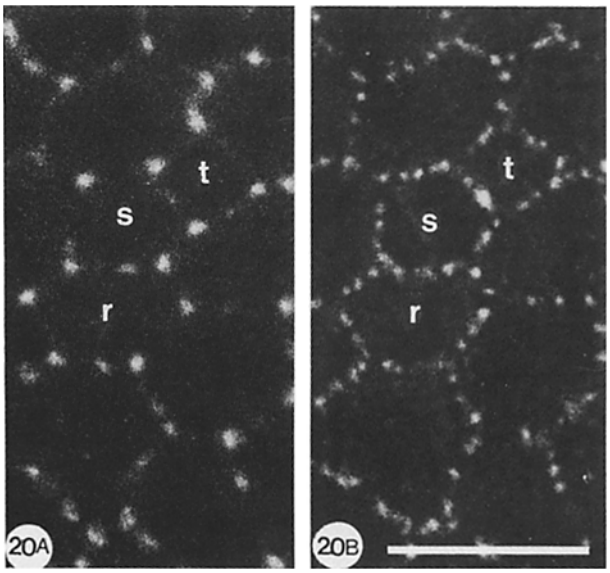

Figure 20. Antibodies to α-actinin (*A*) and desmoplakin (*B*) label different plaques at the lateral cell border of rat prostatic epithelium. Some identical cells are labeled with *r*, *s*, and *t*. Bar, 10 μm.

brane (Fig. 17). The α-actinin (actin and vinculin)–containing type II plaques, on the other hand, had the tendency to form clusters of irregular shape and dimensions. These clusters resembled the irregularly shaped patches and streaks visualized with phalloidin and antibodies to α-actinin in tangential sections (Figs. 12 and 15). Comparison of the two graphs again convincingly showed that both types of plaques are spatially separated from each other. When both types of plaques were printed with different colors in the same reconstruction (not shown), virtually no "black spots" were seen which would have indicated co-localization of the two colors (plaques) in one place.

Squamous Epithelium

To study whether the actin-, α-actinin-, and vinculin-containing plaques also occur in other types of epithelial cells, comparative studies were done on the squamous epithelium of the mouse cornea as well as rat tongue and skin. As shown in Figs. 23–25, antibodies to actin, α-actinin, and vinculin displayed a preferential affinity for the boundaries of corneal epithelial cells. At closer examination typical interruptions of

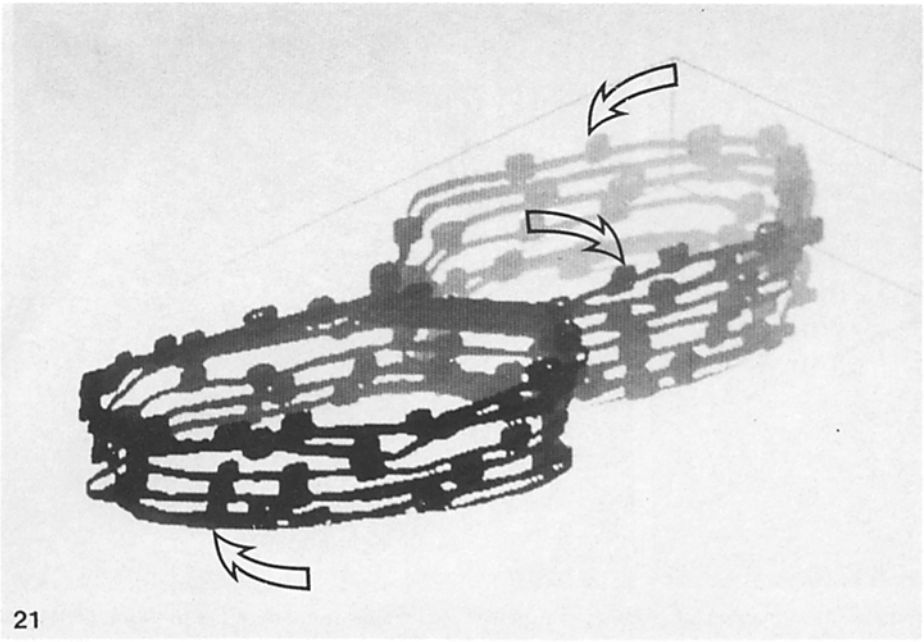

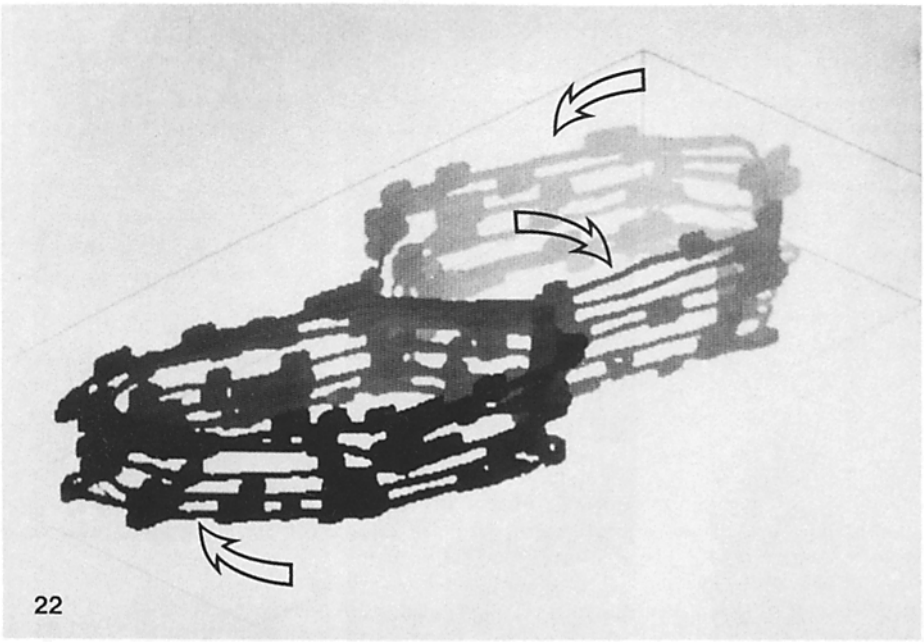

Figures 21 and 22. Three-dimensional computer reconstruction that illustrates the distribution of type I desmosomes (Fig. 21) and the α-actinin (actin, vinculin)–containing plaques (Fig. 22) along the membrane of two adjacent human intestinal epithelial cells reconstructed from seven serial sections 300-nm thick. The sections had been sequentially stained with antibodies to desmoplakin and α-actinin. Photographs were enlarged to a final magnification of 8,000. Subsequent sections were aligned under visual control using an overlay display of structures in neighboring cells. Three-dimensional reconstruction was obtained by a computer graphic system (IBAS, Kontron, Munchen, FRG) using a program developed for computer graphics in neurobiology (46) and modified for the present purpose. The two types of plaques are spatially separated from each other (for instance see places indicated by arrows). The α-actinin-containing plaques tend to form clusters (refer to text).

the immunostain were seen, which were less obvious for the actin stain. Identical results were obtained with squamous epithelium of the rat tongue and skin (not shown). This indicates that type II plaques may represent a cell junction common to different types of epithelial cells.

Discussion

The present study indicates a new type of desmosome-like junction (type II plaques) distributed along the entire lateral plasma membrane of intestinal and prostatic epithelium. The type II plaques clearly differed from the classical type of tonofilament (intermediate filament)–associated spot desmosome (13) by (*a*) considerably lower electron density of the membrane-associated plaque material, (*b*) poorly stained material across the intercellular cleft, (*c*) absence of tonofilaments in association with the plaques, and (*d*) association of the plaques with microfilaments. In a previous study on the cytoskeleton in exocrine gland cells (12), we have shown that microfilaments associated with multiple focal sites along the lateral plasma membrane are actin-containing filaments as determined by decoration with heavy meromyosin. It is proposed that the type II plaques represent a second set of spot desmosomes that are linked to the actin filament system.

The dense plaque material of the type II plaques was always arranged symmetrically, i.e., the membrane-associated densities in one cell were accompanied by a similarly sized density located at the opposing membranes of the neighboring cells. This symmetrical arrangement of densities indicates some kind of communication between the interacting membranes via the intercellular cleft. Intercellular communication is most probably mediated by the poorly stained filamentous material

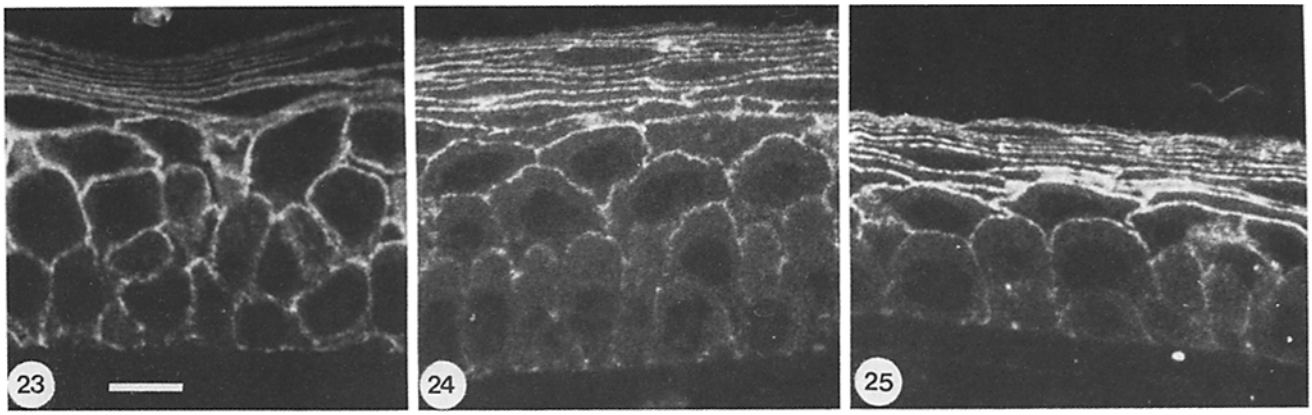

Figures 23–25. Plastic sections of the mouse corneal epithelium stained with anti-actin (Fig. 23), anti-α-actinin (Fig. 24), and anti-vinculin (Fig. 25). Note association of actin, α-actinin, and vinculin with the cell boundaries. Interruptions of the stain are best seen in the sections stained with antibodies to α-actinin and vinculin. Bar, 10 μm.

observed in the intercellular cleft. Recent immunocytochemical studies on the intestinal epithelium indicated the presence of uvomorulin, an embryonic adhesive glycoprotein, in the intercellular space of the zonula adherens and along the lateral plasma membrane (3). Uvomorulin appears to be absent from type II desmosomes (3) and thus may be discussed as a possible candidate for intercellular adhesion at the level of both types of actin-associated junctions, i.e, the zonula adherens and the type II plaques.

Several lines of evidence strongly indicate the association of type II plaques with actin, α-actinin, and vinculin. First, vinculin is a protein confined to particular actin filament membrane associations in various cell types in vitro and in situ (19, 24, 29). α-Actinin, the actin filament cross-linking protein of the muscular Z-line, is also a characteristic component of plasmalemmal anchoring sites of actin filaments (19, 24, 29). It is reasonable, therefore, that the actin-, vinculin-, and α-actinin-containing plaques associated with the lateral cell surface represent places where actin filaments are attached to the plasma membrane. Since type II plaques were the only well-defined plaque-like structures at the lateral plasma membrane associated with actin-like filaments, it is most likely that these sites are identical to the plaques labeled with phalloidin and antibodies to actin, vinculin, and α-actinin. Second, previous studies on the ultrastructural distribution of α-actinin in the intestinal brush border indicated α-actinin-like label at interdigitated parts of the lateral cell boundary (21). As shown in this study, these interdigitated parts are particularly rich in type II desmosomes. Third, antibodies to actin, α-actinin, and vinculin did not bind to type I desmosomes. This was most convincingly seen in three-dimensional reconstructions of parts of the cell wall labeled with antibodies to desmoplakin and α-actinin. Thus, type I desmosomes are not the site of actin, α-actinin, and vinculin. Fourth, type I desmosomes were found in high density in the apical half of the intestinal epithelium and were rather sparse in the basal half of the cells (Fig. 17). Type II plaques, on the other hand, were found in equal density along the entire lateral plasma membrane as were the actin-, α-actinin-, and vinculin-containing plaques (Figs. 12–16).

In previous studies on the ultrastructural organization of the intestinal epithelium (27) and the prostate gland (2), type II plaques have not been demonstrated, most probably because of the very low electron density of the cytoplasmic plaques. In the differentiated prostate epithelium of the dog type I desmosomes, "100F desmosomes" were claimed to be absent, while "70F desmosomes" were said to be the only type of spot desmosome in these cells (33). However, the figures shown in that study illustrate typical I desmosomes. The term "70F macula adherens" was originally introduced by McNutt and Weinstein (32) to discriminate in the developing heart between the typical type I desmosome ("100F macula adherens") and the plaque-like units that constitute the fascia adherens ("70F macula adherens"). Spot desmosomes which do not neatly fall into the classification scheme for adherentes junctions, i.e., macula, fascia and zonula" (32) have been described to occur between embryonic and tissue culture cells as well as between various nonepithelial cell types in situ (for review, see reference 32). Recent studies on such a "desmosome-like junction" (40) between Sertoli cells and germ cells in the mammalian testis have demonstrated actin-like filaments (binding heavy meromyosin) in association with these junctions (44). Immunofluorescence studies indicated α-actinin at these sites (16). Although no data are available regarding the co-localization of actin and α-actinin as well as the demonstration of vinculin at these desmosome-like junctions in Sertoli cells, it is tempting to suggest that these nonepithelial spot desmosomes are related to the type II plaques of epithelial cells.

Type II plaques are associated with the major proteins that are only found at sites of the plasma membrane thought to be involved in intercellular adhesion (zonula adherens, fascia adherens) or in adhesion between the cell surface and the extracellular matrix (focal contacts, dense patches of smooth muscle, "costameres" of striated muscle, postsynaptic densities of the motor endplate). Thus, type II plaques appear to belong to a family of related junctions that appear to be important for cellular adhesion. In contrast to type I desmosomes, which are mainly confined to true epithelial cells (7, 17), type II plaques may be regarded as a more widespread type of desmosome developed between both epithelial and nonepithelial cells.

We are grateful to Dr. Wagner, M. Kirsch, and E. Wagner for their help in setting up three-dimensional computer graphs. The skillful technical assistance of C. Gerhardt, H. Schneider, and R. Corazza is gratefully acknowledged.

This work was supported by the Deutsche Forschungsgemeinschaft (Dr 91-4-1, 91-4-3).

Received for publication 28 August 1985, and in revised form 26 December 1985.

References

1. Alberts, B., D. Bray, J. Lewis, M. Raff, K. Roberts, and J. Watson. 1983. Molecular Biology of the Cell. Garland Publ., New York. 1146 pp.

2. Aumüller, G. 1979. Prostate gland and seminal vesicle. *In* Handbuch der mikroskopischen Anatomie des Menschen Vol. VII/6. A. Oksche and L. Vollrath, editors. Springer Verlag, Berlin, Heidelberg, New York. 380 pp.

3. Boller, K., D. Vestweber, and K. Kemler. 1985. Cell-adhesion molecule uvomorulin is localized in the intermediate junctions of adult intestinal epithelial cells. *J. Cell Biol.* 100:327–332.

4. Bretscher, A., and K. Weber. 1978. Localization of actin and microfilament-associated proteins in the microvilli and terminal web of the intestinal brush border by immunofluorescence microscopy. *J. Cell Biol.* 79:839–845.

5. Burgess, D. R. 1982. Reactivation of intestinal epithelial cell brush border motility: ATP-dependent contraction via a terminal web contractile ring. *J. Cell Biol.* 95:853–863.

6. Burnette, W. N. 1981. "Western blotting" : electrophoretic transfer of proteins from sodium dodecyl sulfate-polyacrylamide gels to unmodified nitrocellulose and radiographic detection with antibody and radioiodinated protein A. *Anal. Biochem.* 112:195–203.

7. Cowin, P., D. Mattey, and D. Garrod. 1984. Distribution of desmosomal components in the tissues of vertebrates, studied by fluorescent antibody staining. *J. Cell Sci.* 66:119–132.

8. Craig, S. W., and J. V. Pardo. 1979. Alpha-actinin localization in the junctional complex of intestinal epithelial cells. *J. Cell Biol.* 80:203–210.

9. Drenckhahn, D., M. Frotscher, and H. W. Kaiser. 1984. Concentration of F-actin in synaptic formations of the hippocampus as visualized by staining with fluorescent phalloidin. *Brain Res.* 300:381–384.

10. Drenckhahn, D., and U. Groschel-Stewart. 1980. Localization of myosin, actin, and tropomyosin in rat intestinal epithelium: immunohistochemical studies at the light and electron microscope levels. *J. Cell Biol.* 86:475–482.

11. Drenckhahn, D., H. D. Hofmann, and H. G. Mannherz. 1983. Evidence for the association of villin with core filaments and rootlets of intestinal epithelial microvilli. *Cell Tissue Res.* 228:409–414.

12. Drenckhahn, D., and H. G. Mannherz. 1983. Distribution of actin and the actin-associated proteins myosin, tropomyosin, alpha-actinin, vinculin, and villin in rat and bovine exocrine glands. *Eur. J. Cell Biol.* 30:167–176.

13. Farquhar, M. G., and G. E. Palade. 1963. Junctional complex in various epithelia. *J. Cell Biol.* 17:375–412.

14. Faulstich, H., H. Trischmann, and D. Mayer. 1983. Preparation of tetramethylrhodaminyl-phalloidin and uptake of the toxin into short-term cultured hepatocytes by endocytosis. *Exp. Cell Res.* 144:73–82.

15. Feramisco, J. R., and K. Burridge. 1980. A rapid purification of α-actinin, filamin and a 130,000-dalton protein from smooth muscle. *J. Biol. Chem.* 255:1194–1199.

16. Franke, W. W., C. Grund, A. Fink, K. Weber, B. M. Jokusch, H. Zentgraf, and M. Osborn. 1978. Location of actin in the microfilament bundles associated with the junctional specialization between Sertoli cells and spermatids. *Biol. Cell.* 31:7–14.

17. Franke, W. W., R. Moll, H. Mueller, E. Schmid, C. Kuhn, R. Krepler, U. Artlieb, and H. Denk. 1983. Immunocytochemical identification of epithelium-derived human tumors with antibodies to desmosomal plaque proteins. *Proc. Natl. Acad. Sci. USA.* 80:543–547.

18. Franke, W. W., S. Winter, Ch. Grund, E. Schmidt, D. L. Schiller, and E.-D. Jarasch. 1981. Isolation and Characterization of desmosome-associated tonofilaments from rat intestinal brush border. *J. Cell Biol.* 90:116–127.

19. Geiger, B. 1983. Membrane-cytoskeleton interaction. *Biochim. Biophys. Acta.* 737:305–341.

20. Geiger, B., A. H. Dutton, K. T. Tokuyasu, and S. J. Singer. 1981. Immunoelectron microscope studies of membrane-microfilament interactions: distribution of α-actinin, tropomyosin, and vinculin in intestinal epithelial brush border and chicken gizzard smooth muscle cells. *J. Cell Biol.* 91:614–628.

21. Geiger, B., K. T. Tokuyasu, and S. J. Singer. 1979. Immunocytochemical localization of α-actinin in intestinal epithelial cells. *Proc. Natl. Acad. Sci. USA.* 76:2833–2837.

22. Gorbsky, G., and M. S. Steinberg. 1981. Isolation of the intercellular glycoproteins of desmosomes. *J. Cell Biol.* 90:243–248.

23. Groschel-Stewart, U., S. Ceurremans, I. Lehr, C. Mahlmeister, and E. Paar. 1977. Production of specific antibodies to contractile proteins, and their use in immunofluorescence microscopy. II. Specific and species-non-specific antibodies to smooth and striated chicken muscle actin. *Histochemistry.* 50:271–279.

24. Groschel-Stewart, U., and D. Drenckhahn. 1982. Muscular and Cytoplasmic Contractile Proteins. *Collagen Relat. Res.* 2:381–463.

25. Hirokawa, N., and J. E. Heuser. 1981. Quick-freeze, deep-etch visualization of the cytoskeleton beneath surface differentiations of intestinal epithelial cells. *J. Cell Biol.* 91:399–409.

26. Hirokawa, N., T. C. S. Keller, R. Chasan, and M. Mooseker. 1983. Mechanism of brush border contractility studied by the quick-freeze, deep-etch method. *J. Cell Biol.* 96:1325–1336.

27. Hull, B., and L. A. Staehelin. 1979. The terminal web. A reevaluation of its structure and function. *J. Cell Biol.* 81:67–82.

28. Laemmli, U. K. 1970. Cleavage of structural proteins during the assembly of the head of bacteriophage T_4. *Nature (Lond.).* 227:680–685.

29. Mangeat, P., and K. Burridge. 1984. Actin-membrane interaction in fibroblasts: what proteins are involved in this association. *J. Cell Biol.* 99(1, Pt. 2):95s–103s.

30. Maupin, P., and T. D. Pollard. 1983. Improved preservation and staining of HeLa actin filaments, clathrin-coated membranes, and other cytoplasmic structures by tannic acid-glutaraldehyde-saponin fixation. *J. Cell Biol.* 96:51–62.

31. Mayor, H. D., J. C. Hampton, and B. Rosario. 1961. A simple method for removing the resin from epoxy-embedded tissue. *J. Biophys. Biochem. Cytol.* 9:909–910.

32. McNutt, M. S., and R. S. Weinstein. 1973. Membrane ultrastructure at mammalian intercellular junctions. *Prog. Biophys. Mol. Biol.* 26:45–101.

33. Merk, I. B., I. Leav, P. W. L. Kirvan, and P. Ofner. 1980. Effects of estrogen and androgen on the ultrastructure of secretory granules and intercellular junctions in regressed canine prostate. *Anat. Rec.* 197:111–132.

34. Mooseker, M. S., E. M. Bonder, K. Z. Conzelman, D. J. Fishkind, C. L. Howe, and T. C. S. Keller III. 1984. Brush border cytoskeleton and integration of cellular functions. *J. Cell Biol.* 99(1, Pt. 2):104s–112s.

35. Mooseker, M. S., T. D. Pollard, and K. Fujiwara. 1978. Characterization and localization of myosin in the brush border of intestinal epithelial cells. *J. Cell Biol.* 79:444–453.

36. Overton, J. 1974. Cell junctions and their development. *Prog. Surf. Sci. Membr. Sci.* 8:161–208.

37. Pardo, J. V., J. D. Siliciano, and S. W. Craig. 1983. A vinculin-containing cortical lattice in skeletal muscle: transverse lattice elements ("costameres") mark sites of attachment between myofibrils and sarcolemma. *J. Cell Biol.* 80:1008–1012.

38. Pease, D. C., and S. Molinari. 1960. Electron microscopy of muscular arteries; pial vessels of the cat and monkey. *J. Ultrastruct. Res.* 3:447–468.

39. Rodewald, R., S. B. Newman, and M. J. Karnowsky. 1976. Contraction of isolated brush borders from the intestinal epithelium. *J. Cell Biol.* 70:541–554.

40. Russell, L. 1977. Desmosome-like junctions between Sertoli cells and germ cells in the rat testis. *Am. J. Anat.* 148:301–312.

41. Skerrow, C. J., and A. B. Matoltsy, 1974. Isolations of epidermal desmosomes. *J. Cell Biol.* 63:515–523.

42. Staehelin, L. A. 1974. Structure and function of intercellular junctions. *Intl. Rev. Cytol.* 39:191–283.

43. Talian, J. C., J. B. Olmsted, and R. D. Goldman. 1983. A rapid procedure for preparing fluorescein-labeled specific antibodies from whole antiserum: its use in analyzing cytoskeletal architecture. *J. Cell Biol.* 97:1277–1282.

44. Toyama, Y. 1976. Actin-like filaments in the Sertoli cell junctional specializations in the swine and mouse testis. *Anat. Rec.* 186:477–492.

45. Tramu, G., A. Pillez, and J. Leonardelli. 1978. An efficient method of antibody elution for the successive or simultaneous localization of two antigens by immunocytochemistry. *J. Histochem. Cytochem.* 26:322–324.

46. Wagner, H.-J., and P. T. Speck. 1985. Computer graphics in neurobiology. *Eur. J. Cell Biol.* 36(Suppl. 7):70. (Abstr.)